Excited state charge separation in symmetrical alkenes

Zijlstra, Robert Wiebo Johan

Theoretical Descriptions of the Sudden Polarization Effect:

The Intramolecular Driving Force Revisited

2.1 Introduction

As early as 1932, Robert Mulliken published a theoretical description of the quantum chemistry of the double bond[1], in which he described ground and excited states of planar and perpendicular ethylene ($R_{1\text{-}4}$ = H, see figure 2.1) in terms of point group symmetry.

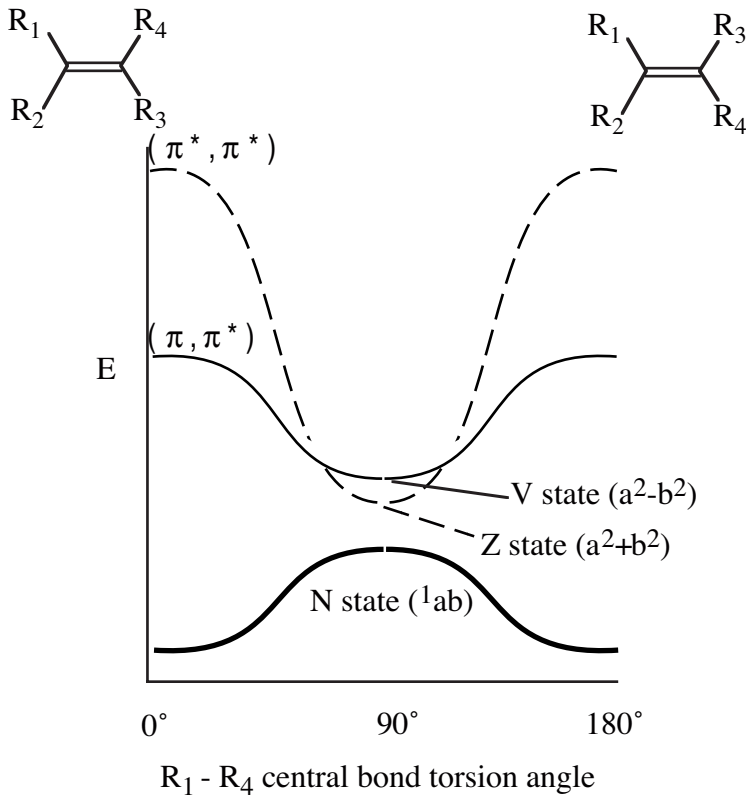

Figure 2.1 Schematic representation of the vacuum potential energy surfaces of the electronic singlet states of interest in (symmetrical) ethylenes.

He predicted the relaxed nuclear geometry of the π,π* state to be (near)-perpendicular, which has distinctive implications for the existing electronic states at this geometry (figure 2.1).

At the perpendicular geometry, the overlap between the two p orbitals at carbon centers a and b is (close to) zero, and as a result the exchange interaction between the electrons occupying these orbitals is small. At this geometry, these two atomic orbitals, which have maximum overlap at planar geometries leading to the formation of the 'closed shell' π molecular orbital, can have occupation numbers between 0 and 2 (with the obvious restriction that the sum of both occupation numbers should be exactly 2).

Mulliken demonstrated that for the perpendicular geometry 4 low lying electronic states exist; a singlet and triplet biradical (^{1}ab (N) and ^{3}ab (B)), being nearly degenerate in energy in which p_x(a) and p_y(b) are singly occupied. Due to the fact that the overlap integral S_{ab} is zero at the perpendicular geometry and the difference in energy between the two states is solely governed by the exchange integral K_{ab}, the ^{3}ab state is predicted to be the slightly more stable state (by an amount of $2K_{ab}$), as dictated by Hund's rule. The other two states were estimated to lie approximately 1 eV higher in energy, 'originating

from the CH_2^+ and CH_2^- fragments'. These can be written as $p_x(a)^2$ and $p_y(b)^2$ and can be interpreted as zwitterionic states.

Due to the fact that in a non-perturbed (i.e. D_2-symmetrical) wave function both zwitterionic solutions are equally acceptable, the correct representation of these upper two states are the symmetrized linear combinations of the two states (equation 2.1):

$$\Psi \sim p_x(a)^2 \pm p_y(b)^2 \qquad \textbf{(2.1)}$$

These states are commonly referred to as the Z and V states; with coefficients $c_1 = c_2 = {}^1/_2\sqrt{2}$. It is tempting to use the term biradical(oid) in order to label the wave functions described by equation 2.1 in situations where $c_1 \approx c_2$, when the wave function basically consists of a linear combination of the two localized (ionic) closed shell determinants a^2 and b^2 rather than of two unpaired electrons. It should be clear, however, that the term 'biradical' is applicable to the ^{1}ab (N) and ^{3}ab (B) states rather than the states described by equation 2.1, since the term biradical is usually associated with electronic states in which two unpaired, weakly interacting electrons are present[2].
A more appropriate nomenclature of these states based on their behaviour is suggested in chapter 5, where the outcome of an experimental study on the photo-induced excited state dynamics of tetraphenylethylene (TPE) is discussed.

The direct consequence of the excited state behaviour as a result of the shape of the wave functions in equation 2.1 stayed unrecognized until the early seventies. In 1970, Marshall reported remarkable and unexpected polar behaviour in the excited states of several cyclohexenes and cycloheptenes[3], molecules exhibiting only a very small dipole moment in their ground state geometries. Wulfman et al. explained this by suggesting that under a perturbation of, for instance, the electric field of a nearby ion c_1 and c_2 can become unequal[4, 5]. In their words, a catastrophic polarization of the near-perpendicular excited states could occur. The occurrence of a 'catastrophic' polarization results in wave function representations for the two excited states for which the two electrons become localized at one half of the molecule, thus forming zwitterionic (or polar) states, which was presented as a possible explanation for the observed excited state polarity by Marshall.

This dramatic polarizability of the excited state has been shown to depend critically on the amount of twisting of the central bond[6-12]. It was demonstrated that this behaviour only exists in (close) vicinity of the perpendicular geometries, since the necessary degeneracy between the Z and V states only exists in this region (figure 2.1). The fact that this behaviour only occurs in a confined region of the excited state potential energy surface (PES) is the main reason why it is often referred to as 'sudden polarization', as suggested by Bonacic-Koutecky[6].

2.2 Theoretical Description of Relevant Methods

In this section, an overview will be given of the computational models for the work presented in this chapter and for studying the sudden polarization effect in general. More extensive descriptions can be found in the documents referred to and references therein.

The calculation of electronic properties of molecular systems are usually based on quantumchemical descriptions of some sort. In such approaches the aim is to find an approximate solution of the Schrödinger equation for the N electrons in the system[13, 14]. This can be done in several ways, but usually the N-electron wave function is expanded in anti-symmetrized products Φ_k of the one-electron functions φ_i (eq. 2.2 and 2.3),

$$\Psi = \sum_k C_k \Phi_k \qquad \textbf{(2.2)}$$

$$\Phi_k = \hat{O}^a (\varphi_p(1)\, \varphi_q(2) .... \ \varphi_s(N)) \qquad \textbf{(2.3)}$$

with Φ_k usually referred to as Slater determinants. A linear combination of Slater determinants that fulfils spin and spatial symmetry constraints is usually referred to as a configuration state function (CSF). The exact solution of the problem is given by the complete (i.e. infinite) expansion of all Slater determinants that can be generated from the one-electron space. Since this solution is unachievable for obvious reasons, approximate solutions to the N-electron problem have to be found.

The simplest and most frequently used approach to approximately solve such an N-electron problem is the Hartree-Fock (HF) or Self Consistent Field (SCF) method; a method aimed to find the orbital solution with the lowest accompanying energy.

In this method the N-electron space is limited to just one Slater determinant, in which case equation 2.2 simplifies to:

$$\Psi = C_0 \Phi^{HF} \qquad \textbf{(2.4)}$$

In HF methods, the electron-electron repulsion is treated in a mean-field way. In many cases, like in the case of organic molecules in their electronic ground state configurations the HF approximation is very reasonable. However, if one is for instance interested in the description of excited states or in calculating the expectation value of an energy with high accuracy, correlated wave functions, in which the various electron-electron repulsions (the so-called electron correlation effects) are explicitly taken into consideration, are required.

In cases where the HF wave function is already a reasonable estimate, an accurate description of the wave function can usually be obtained by employing Configuration Interaction (CI) calculations. An important feature of a CI calculation is that it leaves the reference one-electron functions (orbitals) unchanged, which is why the HF reference wave function needs to be of reasonable quality. Usually, the inclusion of single and double excitations from the reference wave function leads to the retrieval of a large part of the electron correlation effects. This method is known as the Configuration Interaction Singles Doubles (CISD) method:

$$\Psi^{CISD} = C_0 \Phi^{HF} + \sum_{i,\,a} C_i^a \Phi_i^a + \sum_{ij,\,ab} C_{ij}^{ab} \Phi_{ij}^{ab} \qquad \textbf{(2.5)}$$

in which the first sum depicts all configurations generated by single excitations from the HF reference wave function and the second sum depicts all configurations originating

from double excitations. However, in cases where the HF reference provides a qualitatively poor description of the actual wave function, the CISD approach will not yield reliable results and more appropriate methods are needed to accurately describe the wave function.

A better description can be obtained by using the Multiconfigurational SCF (MCSCF) method. This method also includes all nearly degenerate configurations in the reference wave function:

$$\Psi = C_1 \Phi_1 + C_2 \Phi_2 + ... \quad C_i \Phi_i + ... \quad C_m \Phi_m \qquad \textbf{(2.6)}$$

In a MCSCF calculation, the one-electron orbitals are optimized in a SCF type step, thus improving the quality of the reference wave function as well. In such calculations, Ψ can be optimized for a single state, or for a mixture of states. The latter application is commonly reffered to as a state averaged calculation.

An MCSCF wave function can be used as a reference in CI calculations that are capable of including a plurality of reference wave functions. This is particularly useful in cases where the HF method gives a poor description of the N-electron wave function, in which case the CISD method is not the most appropriate method for including electron correlation effects.

Such Multi Reference CI (MRCI) wave functions can be written as an ordering of the external configurations by their number of external electrons:

$$\Psi^{MRCI} = \sum_{m} C_m \Phi_m + \sum_{m,\,a} C_m^a \Phi_m^a + \sum_{m,\,ab} C_m^{ab} \Phi_m^{ab} \qquad \textbf{(2.7)}$$

with m indexing over all configurations in the reference wave function in both equations 2.6 and 2.7. Such CI expansions can yield excellent results, but are quite time consuming, especially if no CSF selection algorithms are applied.

A popular setup of MCSCF wave functions is the so-called Complete Active Space SCF (CASSCF) formalism[15, 16]. In the theoretical summary presented below, the following labels will be used:

- a, b, c,... for secondary (virtual) orbitals
- i, j, k,... for inactive orbitals
- p, q, r and s for general orbitals
- t, u, v,... for active orbitals

The active orbitals are the orbitals which are included in the CAS expansion. Inactive orbitals are the *occupied* orbitals which are excluded from this expansion, whereas secondary (or virtual) orbitals are the *unoccupied* orbitals that are excluded from the CAS. Finally, general orbitals can either be occupied or unoccupied, and can either be active or inactive/secondary orbitals. Within the CASSCF formalism, the orbital space is divided into three subsets:

- the inactive space (i.e. the complete set of inactive orbitals)
- the secondary (or virtual) space (i.e. the complete set of secondary orbitals)

- the active space (i.e. the complete set of active orbitals)

Orbitals in the inactive space stay doubly occupied in all configurations whereas orbitals in the secondary space remain unoccupied. The electrons occupying orbitals in the active space are distributed in all spin and symmetry allowed ways.
In fact, a complete CI is being performed over the active space. This has the additional advantage that, as a result of the completeness of the wave function, orbital rotations (i.e transformations to restore orthogonality) among active orbitals are redundant and can be ignored. This is one of the main reasons why CASSCF wave functions usually converge rapidly.

In CASSCF calculations, the core orbitals are orbitals that typically occupy the inactive space, because they usually have a negligable influence on the correlation energy. It should be emphasized that the CASSCF method is not constructed to provide a good estimate of the electron correlation effects, but to provide an excellent starting point to obtain such estimates with other methods.

A more flexible setup of MCSCF wave functions can be achieved with the Restricted Active Space SCF (RASSCF) approach[17]. This approach embodies five active spaces called RAS1, RAS2 and RAS3 together with an inactive and an external space. The latter two are similar to the inactive and the secondary space in a CAS type description. In the RAS1 space a fixed number of holes is allowed (i.e. the number of electrons allowed to be excited from the RAS1 to either the RAS2 or RAS3) whereas in the RAS3 a fixed number of added electrons (i.e. electrons excited into the RAS3 from either the RAS1 or RAS2) is allowed. Again, in the RAS2 a complete CI expansion is formed. The main advantage of a RASSCF is that it is able to tackle larger systems. Therefore, when practical restrictions prohibit the inclusion of the full orbital set in the active space, it usually provides a better estimate of the electron correlation than a CASSCF approach. However, due to the fact that the wave function is no longer complete in just one active space, the active - active orbital rotations between the three active spaces now have to be included in the method to eliminate the nonorthogonality between the RAS spaces, which was introduced by the orbital optimization steps. As a result, RASSCF type wave functions usually converge much more slowly than CASSCF wave functions due to this inclusion, making RASSCF calculations less accessible.

A way of obtaining an estimate of the correlation energy in a nonvariational manner is by applying Møller-Plessett (MP) perturbation theory[18] on a reference wave function. This theory states that in the case of a dominating RHF wave function, a division of the Hamiltionian can be made:

$$\hat{H} = \hat{H}^{(0)} + \hat{H}^{(1)} \qquad \textbf{(2.8)}$$

In this expression, the zeroth order Hamiltionian is defined as the sum over the one-electron Fock operators:

$$\hat{H}^{(0)} = \sum_{I}^{N} \hat{F}(I) \ , \qquad \hat{F}(I)\ \varphi_i(I) = \varepsilon_i \varphi_i(I) \tag{2.9a}$$

$$\hat{H}^{(0)}\Phi_{HF} = E^{(0)}\Phi_{HF},\ \langle \Phi_{HF} | \hat{H} | \Phi_{HF} \rangle = E^{(0)} + E^{(1)} \tag{2.9b}$$

where I runs over all electrons. In 2.9b, the zeroth order energy is the sum over all occupied orbital energies ε_i, whereas the first order energy is equal to the HF energy.

The application of second order perturbation theory (MP2) provides an estimation of the correlation energy and first order wave function in the following manner:

$$E^{(2)} = -\sum_{i<j} \sum_{a<b} \frac{\left[\langle \varphi_i \varphi_j | \hat{H}^{(1)} | \varphi_a \varphi_b \rangle \right]^2}{\varepsilon_a + \varepsilon_b - \varepsilon_i - \varepsilon_j} \tag{2.10}$$

$$\Psi^{(1)} = \sum_{i<j} \sum_{a<b} C_{ij}^{ab\,(1)} |\Phi_{ij}^{ab}\rangle \text{ with } C_{ij}^{ab\,(1)} = \frac{\langle \varphi_i \varphi_j | \hat{H}^{(1)} | \varphi_a \varphi_b \rangle}{\varepsilon_a + \varepsilon_b - \varepsilon_i - \varepsilon_j} \tag{2.11}$$

The necessary parts of equations 2.10 and 2.11 can be easily obtained from the preceding RHF reference wave function, which makes MP2 an accessible and straightforward method to obtain an estimate of the electron correlation effects. Extending this theory to multiconfigurational wave functions is not possible, because the partitioning of the Hamiltonian (equation 2.8) cannot be made.

To allow the application of perturbation theory to MCSCF wave functions, other methods have to be used. One such method has been developed by Roos and Andersson. The second-order Complete Active Space Perturbation Theory (CASPT2)[19, 20] requires a CASSCF wave function as reference. From this reference it calculates the remaining electron correlation energy and the first-order estimate of the wave function. In this theory, $\hat{H}^{(0)}$ is a sum of Fock-type one-elctron operators which reduces to the MP operator when a single configuration reference is being used;

$$\hat{H}^{(0)} = \sum_{pq} f_{pq} \hat{E}_{pq} \qquad \text{with } f_{pq} = -\left\langle 0 \left| \left[\left[\hat{H}, a_q^{\dagger} \right], a_p \right]_+ \right| 0 \right\rangle \tag{2.12}$$

where $|0\rangle$ is the CASSCF reference function and $\hat{E}_{pq}$ an excitation operator defined as the product of a creation operator $a_q^{\dagger}$ and an annihilation operator a_p.

The first-order wave function $|\Psi^{(1)}\rangle$ can be constructed in a similar fashion as in the Internally Contracted MRCI (ICMRCI) method[21]. It can be expressed as an internally contracted expansion of all configurations connected to single and double excitations from the CASSCF reference wave function:

$$\left| \Psi^{(1)} \right\rangle = \sum_{pqrs} C_{pqrs} \hat{E}_{pq} \hat{E}_{rs} |0\rangle \tag{2.13}$$

The CASPT2 extension to a CASSCF calculation generally provides a very good estimate of electron correlation effects.

A possible breakdown of perturbation theory based on Fock-type operators can occur if states with a similar expectation value of $\hat{H}^{(0)}$ as the reference wave function exist (so-called intruder states). In these cases, energy differences between the states are near zero which will lead to very small energy denominators in the expressions for $E^{(2)}$ and $C^{(1)}$, leading to the aforementioned breakdown. The best way to avoid this behaviour is to include the near-degenerate states in the reference wave function. However, in cases where this reference is already very large, such inclusions might become unfeasible and other techniques have to be considered. A possible solution can be found in applying level shifting techniques[22]. The use of such techniques has not been required in this thesis and will therefore not be described here.

2.3 Theoretical Investigations on the Sudden Polarization Behaviour of (*D2*-Symmetrical) Ethylenes: History and Approach

The dramatic implication of the near degeneracy of the Z and V states, the polarization catastrophe as suggested by Wulfman and Kumei[4], has initiated a large number of studies concerning the electronic behaviour of the photo-excited states in a wide variety of olefinic compounds in the vicinity of their perpendicular geometry[8, 10, 23-28].

In the first place, since photo-induced alkene isomerization by excitation of one or more double bonds plays an important part in both naturally occurring[29, 30] as well as synthesized compounds[31], several model systems have been investigated to determine the *generality* of the sudden polarization effect in alkenes.

Another motivation has been the determination of the *driving force* behind the occurrence of the polarized, zwitterionic states in these systems. As already mentioned in the opening paragraph, a symmetry lowering perturbation of the wave function is necessary to break the (near-) degeneracy of the two states involved in order to shift their representation towards a zwitterionic form[6, 10, 23].

An important complication of the theoretical description, or at least the interpretation of the theoretical studies dealing with the sudden polarization behaviour is the fact that the Born-Oppenheimer approximation is no longer valid in the vicinity of the crossing between the two potential energy surfaces as the electronic behaviour of these states will be governed by the nuclear motions[32-34]. This leads to an avoided crossing between the two states where the strength of the perturbation will determine the transition probability between the two surfaces[35].

When investigating the literature on the topic of sudden polarization in symmetrical ethylenes, it turns out that only a few studies deal with the theoretical description of this phenomenon[10, 23, 24, 27, 36-38], and most of these studies have been performed on the parent alkene ethylene, in which case the symmetry breaking by means of an internal pyramidalization of one of the CH_2 centers is believed to be the driving force behind the occurrence of large excited state dipole moments. The influence of

substituents on the pyramidalization process has hardly been studied, and in the few reported cases, like the work of Bonacic-Koutecky et al. on propylene[24] the methyl group containing carbon has been excluded from the pyramidalization process.

There are two main reasons for this fact. First of all, the use of computationally challenging correlated wave functions is necessary to properly describe the (near-) degeneracy of the Z and V states of ethylenes. In addition, a sometimes ignored bottleneck in such calculations is the (lack of) molecular symmetry in the excited states of interest. Although the ethylenic nuclear framework in the near perpendicular region of interest still exhibits C_{2h} or even D_{2d} symmetry at the perpendicular geometry, the excited states of interest do not fit into this point group for the following reason.

In D_2 symmetry, the plane of symmetry perpendicular to the C-C bond conflicts with the symmetry broken zwitterionic determinants a^2 and b^2 which form the Z and V states (figure 2.4). This can be understood in the following manner. In C_1 symmetry, the charge symmetrical representations of the excited states of interest can be formed by a linear combination of the two zwitterionic determinants a^2 and b^2. For a^2, the inner shell electrons will polarize towards the opposite carbon atom as a result of the localization of the two outer shell electrons on the first carbon center, thus causing additional relaxation in the charge distribution of this particular determinant. Obviously, the same holds for the b^2 determinant. In higher symmetry like D_2 symmetry, the $a^2 \pm b^2$ states each have to be formed within a symmetrical subset of orbitals. As a result, the aforementioned (low-symmetrical) inner shell relaxation effects cannot be reproduced (unless extensive orbital expansions are included in the active space), which leads to a severe overestimation of the energy of these states.

A description and a prime example of this effect are given in the pioneering work by Broer[39], who showed that the correct description of the core excitations in N_2 is extremely difficult when using truncated active spaces in combination with the full $D_{\infty h}$ symmetry of the molecule. In fact, a non-orthogonal configuration interaction (NOCI) calculation[39] on the two symmetry broken localized excitations from N_a and N_b had to be performed to approximate the experimental excitation energy.

In practice, this means that, in the case of ethylene, only a C_2 symmetry, using the C-C bond as rotation axis, or a C_s symmetrical representation, using the mirror plane coinciding with the C-C bond, is acceptable since this is the highest symmetry representation including the inner shell relaxation effects without having to extend the active space. For now, it should be reminded that the restrictions on the imposable symmetry imply a rapid increase in the dimensions of the wave function with increasing molecular size, thus limiting the application of 'sophisticated' computational methods to modestly sized molecules.

The second fundamental problem arising from the desire to describe such heavily interacting potential energy surfaces (apart from the breakdown of the Born-Oppenheimer approximation) is that the choice of the configurational active spaces (i.e. the number of electrons and orbitals to be included in the computation) should be highly balanced to prevent unphysical polarization in the ethylenic excited states of interest. If one of the two halves of the molecule contributes more virtuals (i.e unoccupied orbitals) to the active space in the calculation, the zwitterionic determinant at this half can become 'more correlated' than on the other half, where a smaller number of active space orbitals are present. Even a small inbalance can already lead to heavily polarized excited states in

regions where the Z and V potential energy surfaces are near degenerate. Especially MCSCF wave functions suffer from this problem[10, 14] due to the fact that the orbital optimization step in MCSCF calculations tends to disturb the delicate balance between the two molecule halves involved (*vide infra*).

In addition, variations in the size of perfectly balanced active spaces as well as basis set quality can have a distinct effect on the excited state behaviour on symmetry breaking. The latter effect is of course not unexpected, since this excited state electronic behaviour can be explained in terms of polarizability, and basis set quality as well as the size of the expansion (or better: active space) of a correlated wave function have a marked effect on this property.

However, the aforementioned difficulties in describing the sudden polarization effect in physically correct way can best be tackled by the use of CI wave functions. Paradoxically, the main reason for the strength of the CI method is caused by one of its restrictions: the quality and applicability of a CI wave function mainly depends on the quality of its reference wave functions.

This is caused by the fact that the CI method is solely based on the 'input orbitals' of the reference wave function. As a result, a complete symmetrical wave function will guarantee symmetrical Z and V states for the obvious reason that 'polar' configuration state functions on either side of the double bond will contribute with equal weights to the optimized CI wave function ensuring the physically correct unpolarized excited states in vacuo. This straightforward advantage is the main reason why the bulk of the computational work on the topic of ethylenic excited states sofar has been on the basis of CI wave functions.

Several theoretical studies using CI techniques to study the sudden polarization effect in ethylene in the vicinity of the crossing of the Z and V potential energy surfaces (PES) have been presented[9, 10, 12, 23]. For a couple of them, their outcomes and conclusions have been accepted as an accurate or even a general description of the driving forces behind the sudden polarization phenomenon in symmetrical alkenes[10, 23]. Both these studies have focussed on a combination of twisting along the central bond and selective pyramidalization of one of the two CH_2 centers.The first report described a CISD study by Brooks and Schaeffer[III] in 1979[10], who used the orbitals of the ^1ab N state in the standard Dunning Huzinaga (DZV) basis as reference. These orbitals were generated in a constrained SCF procedure in which the weights of the a^2 and b^2 configurations were forced to be equal even for C_s geometries. It was shown that upon selective (i.e. one-sided) pyramidalization, the $a^2 + b^2$ state (i.e. the Z state) became more stable in comparison with its unpyramidalized nuclear configuration. Also, upon progressive pyramidalization, it exhibited an increasing dipole moment, with the two unpaired electrons effectively located on the pyramidalized carbon center. This dipole moment (along the C-C bond; μ_z) reached a maximum value of 3.3 D. On the other hand, the V state was increasingly destabilized on progressive pyramidalization with a maximum μ_z of similar magnitude but of opposite sign, indicating that the two elecrons reside on the unpyramidalized carbon center in this state. Furthermore, when using truncated CI spaces (i.e. a CI expansion allowing only the two biradical electrons to excite into the virtual space of the twisted ethylene) the calculated dipole moments are much larger than in the case of the all valence CISD, showing the need for a balanced CISD expansion, in which other configurations than the a^2, b^2 states apparently play an unusually important role. It

was suggested that internal symmetry breaking is indeed the driving force in the sudden polarization of ethylenes. The amount of polarization was suggested to be correlated with the coupling matrix in equation 2.14 in a qualitative fashion, with E_a and E_b the energies of the two ionic forms of ϕ_a and ϕ_b and H_{ab} representing the exchange and overlap terms betweem them.

$$H = \begin{pmatrix} E_a - E & H_{ab} \\ H_{ab} & E_b - E \end{pmatrix} \qquad \textbf{(2.14)}$$

Especially in the vicinity of the 90˚ (perpendicular) twist angles, H_{ab} merely consists of the small exchange term K_{ab}, and excessive mixing can take place as a result of only small perturbations of the symmetrical wave function.

This qualitative description has been refined in a more elaborate study by Buenker, Bonacic-Koutecky and Pogliani[23], in which the simultaneous torsion and pyramidalization of ethylene was studied by means of multi reference CI techniques using configuration selection. Even though the findings were roughly the same as those of Brooks et al. some additions were made to the mechanistical picture. First of all, it was observed that the amount of polarization of the Z and V states depended critically on the choice of reference orbitals. Even though no experimental values were present, which prohibited verification of the computational findings, it was suggested that the use of the MO's of the ^{3}ab state as reference gave the most reliable results.

It was suggested that the minimum energy configuration for the S_1 state was found at the very large pyramidalization angle of 60˚. Furthermore, the maximum polarization was found around 82˚ rather than around the perpendicular geometry. This was quantitatively explained as follows: the amount of polarization depends on the coupling matrix as described in equation 2.14. With respect to the two coefficients in equation 2.1, which ratio describes the amount of mixing of the localized determinants, this can be combined in the following way according to first-order perturbation theory:

$$\left| \frac{c_1}{c_2} \right| \approx \left| \frac{H_{12}}{\Delta E} \right| \qquad \textbf{(2.15)}$$

Therefore, at the 82˚ geometry, where the Z and V state become degenerate, large fluctuations in polarization can occur as a result of minor changes in the off-diagonal matrix element H_{12} only. At the perpendicular geometry, ΔE is large with respect to H_{12}, and polarization effects become less pronounced as a result of that. Even though the results and conclusions in the above described papers are both significant and highly valuable, some puzzling questions remain. Let's for instance take a look at figure 2.2.

It demonstrates the effect of pyramidalization on the internuclear distance of the functional groups attached to the carbon. Obviously, increasing pyramidalization leads to a decreasing internuclear distance between the groups attached to the pyramidalized carbon centre, and figure 2.2 clearly shows that this distance becomes increasingly smaller for larger (or bulkier) groups. This is of course a simplified picture, because the C-R bond lengths will be somewhat longer than that of a C-H bond, thus (partially) counteracting this effect on internuclear distance. However, it does raise the question whether

pyramidalization will always lead to more stable, zwitterionic forms of the ethylenic excited states at near-perpendicular geometries in systems, regardless of the size of the functional groups are attached to the pyramidalized carbon centre.

In practice, some larger alkenes have been studied experimentally and some intriguing results have been obtained. For instance, spectroscopical investigations on tetraphenylethylene (TPE) in the condensed phase[40-43] have indicated that especially in non-polar solvents a considerable fraction of the excited state population is non-polarized, indicating possible limitations of the validity of the generalized picture of sudden polarization by selective pyramidalization. This observation justifies a more detailed study on the effects of pyramidalization on larger ethylenes.

To accomodate this need, in this chapter the outcome of an exploratory study on a couple of small ethylenes (ethylene, tetramethylethylene) at the CASPT2 level of theory will be presented, despite the aforementioned drawbacks of MCSCF methods when studying the sudden polarization effect.

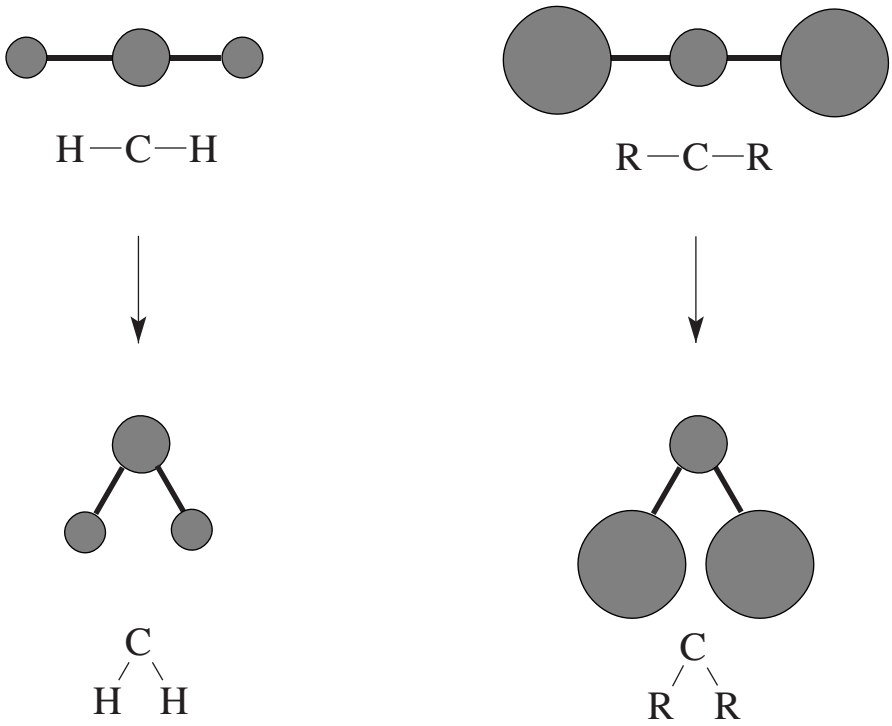

Figure 2.2 Schematic representation of pyramidalization of a CH_2 and a more bulky CR_2 group (viewed alongside the olefenic bond)

The main reason for choosing a MCSCF based approach is that no other appropriate computational tools were available to perform the calculations involving tetramethylethylene (TME). As already mentioned, the use of MCSCF wave functions on studying the sudden polarization effect has some serious limitations with regard to the correct representation of the charge distributions of the electronic states involved. For instance, at the D_{2d} (i.e. unpyramidalized perpendicular) geometry, the electronic representations of the (ionic) Z and V states of ethylene are of a physically incorrect symmetry broken form. This obviously asks for a critical look at the outcome, since the accompanying energies can be unrealistic as well, even though the near-degeneracy of the

two states of interest allows for large polarizations without significantly altering the state energy.

A comparison with the earlier mentioned pioneering work of Brooks and Schaeffer[III] on ethylene[10] will be made to check the validity of the obtained results. It will be shown that even though the obtained dipole moments belonging to the symmetry broken solutions of the Z and V state are clearly unrealistic in the sense that perfectly symmetrical nuclear configurations yield large dipole moments (opposed to results obtained when using CI methods, in which case these configurations have perfectly zero dipole moments), the obtained CASPT2 potential energy surfaces are actually in good agreement with the Brooks' CI results, even at larger pyramidalization angles. Therefore, the results of a pyramidalization study on tetramethylethylene (TME) at its perpendicular geometry will be presented, in order to determine whether the pyramidalized perpendicular geometry of the Z state is still the most stable excited state geometry in cases where the ethylenic double bond carries more sizeable substituents. As explained before, this is a critically important question, since the internal symmetry breaking by one-sided pyramidalization is believed to be the general driving force behind the occurrence of charge separation in symmetrical ethylenes.

2.4 Results and Discussion

The results of the simultaneous torsion and pyramidalization of ethylene and pyramidalization of perpendicular TME will be discussed here. This study has been performed at the CASPT2 level using MOLCAS3.5[44]. In these calculations, the standard Pierloot ANO-s basis[45] of size 4s3p2d on C and 3s2p on hydrogen for ethene and 3s2p1d on carbon and 2s1p on hydrogen for TME has been used. The smaller basis for TME was chosen to reduce computational efforts. All calculations have been performed without imposing symmetry constraints. For ethylene, a CAS of 8 electrons in 12 orbitals has been used. The included occupied orbitals consist of the C-C σ and π bond as well as two H-C-H delocalized orbitals on both sides of the molecule. This selection has been made on the basis of an exploratory RASSCF calculation in which the RAS2 was kept empty and all valence orbitals as well as 20 virtuals were included in the RAS1 and RAS3 respectively, allowing two holes in the RAS1 and 2 electrons in the RAS3. The ethylene geometry used has been identical to the one used by Schaeffer[III] et al.[10] and is depicted in figure 2.3.

Figure 2.3 Adopted ethylene geometry (left) and definition of pyramidalization (or out-of-plane bending) angle ϕ

The TME geometry has been generated in a RHF geometry optimization in the standard 6-31G* basis using Gaussian94. For the CASPT2 calculations, the central C-C bond length was set to 1.416 A after a manual optimization of this bond length at the CASSCF level of theory (see below for details on the CAS) at the TME perpendicular geometry. In this calculation a state averaged wave function with equal weights for the Z and V state was used. The TME active space has been determined by a similar RASSCF procedure as in the ethylene case. Here, an active space of 10 electrons in 10 orbitals has been chosen.

It should be emphasized that these selections have been made by choosing all near-degenerate orbitals from both the occupied and virtual space with the attempt to create a reasonably balanced CAS space. Obviously, better motivated selections could have been made but as already mentioned before, even highly balanced expansions still lead to symmetry broken solutions for the Z and V states so the additional effort was deemed to have a negligible effect. In fact, the current expansions proved to be quite reasonable, since in all unpyramidalized geometries the lowest root (the biradical N state) exhibited near-zero dipole moments at the CASSCF level for both ethylene as well as TME , indicating the balanced nature of the CAS.

Another problem that is frequently encountered when dealing with the electronic spectra of small alkenes is the occurrence of low lying Rydberg states in the spectra, which become 'overcorrelated' in truncated correlation expansions[46-48]. As a result of this, the first excited states incorrectly appear to have Rydberg rather than valence character. For instance, in the case of ethylene it has been demonstrated that large MRCI expansions have to be used to obtain the correct state ordering in the electronic spectrum of the parent alkene[47]. Fortunately, upon twisting away from the planar geometry these Rydberg states destabilize quickly and even very moderate active spaces correctly reproduce the valence nature of the excited states at the geometries of interest in this work.

The CASPT2 calculations were performed in the following manner: first a state averaged CASSCF (with weights 1:1:1) over the three roots of interest (N, Z and V state) has been performed (using a RHF reference as starting orbitals). The thus generated orbitals were used as starting orbitals for the separate CASSCF optimizations of the three roots of interest. In the CASSCF calculations of the Z and V states in the 80-90˚ range some moderate state averaging had to be applied in order to achieve convergence of the calculation. In the case of the Z state ($a^2 + b^2$), a small weight (10%) of the N state needed to be included to ensure convergence of the calculation. For the V state ($a^2 + b^2$), the Z state had to be mixed in (with a weight of maximum 20%) to prevent alternating charge hopping between the two carbon centres in two subsequent SCF cycles.

Subsequently, a CASPT2 calculation was performed to determine the contribution of the inactive and secondary spaces to the electron correlation energy. As already mentioned in section 2.2, this usually is a necessary step in order to get a good estimate of the electron correlation effects when choosing a CASSCF based approach. At this point, it should be mentioned that in all cases the CASPT2 calculations completed without the occurrence of intruder states in the CASPT2 wave functions. This was established by checking the magnitude of the weight of the original CASSCF wave function in the final CASPT2 result. In all cases it was large enough to justify this conclusion.

Two angles were varied in the ethylene calculations; the rotation angle α, which has been varied over a 60-90˚ range with 5 degree increments (with the exclusion of the 65˚

geometry), and the pyramidalization angle ϕ, which has been varied from 0 to 30˚, with 10˚ increments also including ϕ = 5˚ (see also figure 2.4). For TME, ϕ was varied with 10˚ increments at the perpendicular geometry only. More elaborate studies on TME including other values of α had to be abandoned due to lack of time. The resulting CASSCF and CASPT2 energies are given in table 2.1 and 2.2. These results have been visualized in figure 2.4.

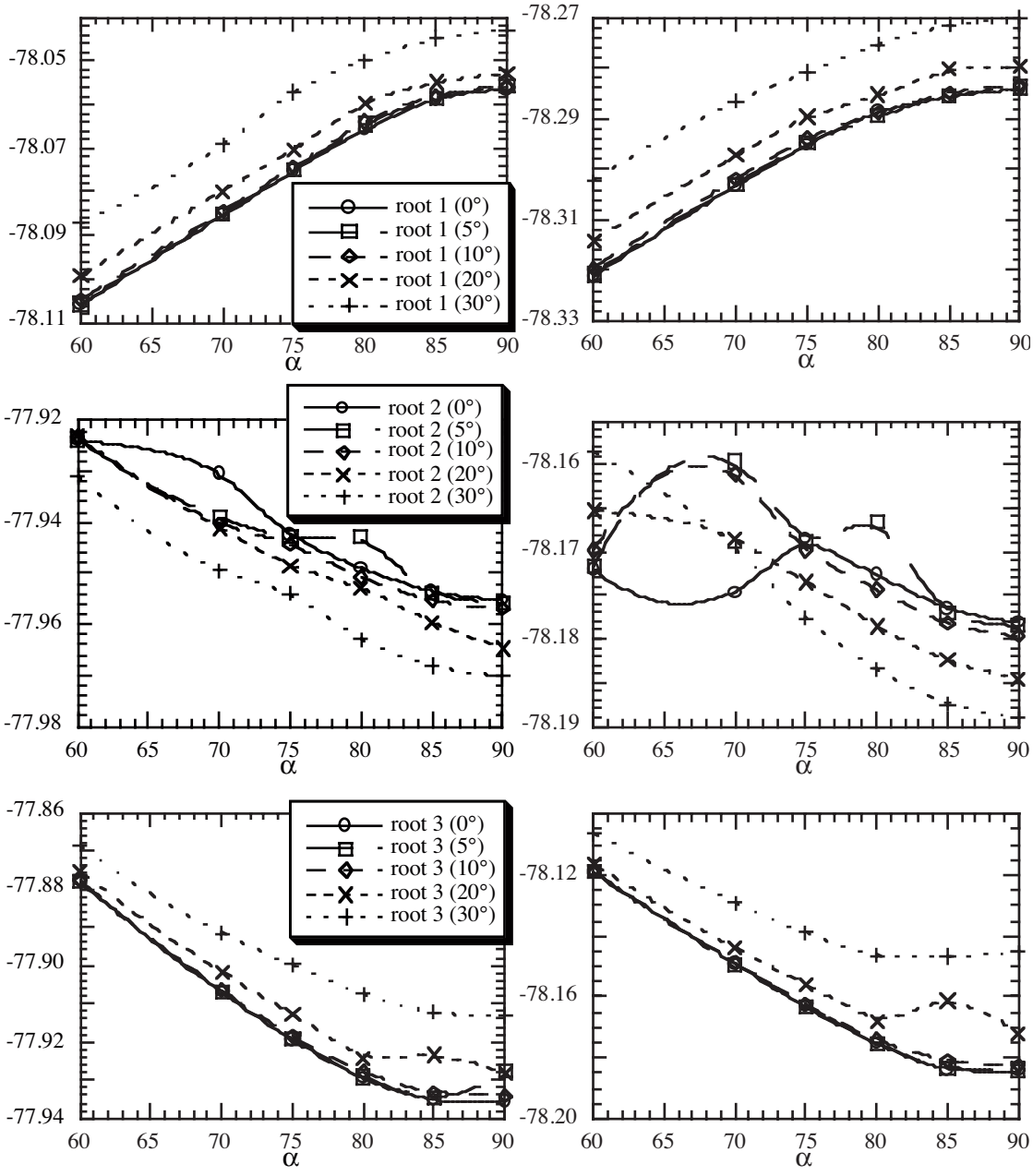

Figure 2.4 CASSCF (left plots) and CASPT2 (right plots) potential energy surfaces (a.u.) of root 1 (top), root2 (middle) and root 3 (bottom) of ethylene at various values of ϕ (in brackets)

α/ϕ	root 1	root 2	root 3
60/0	-78.105921	-77.923929	-77.878015
70/0	-78.085399	-77.930377	-77.906869
75/0	-78.075151	-77.942382	-77.919433
80/0	-78.065764	-77.948938	-77.929560
85/0	-78.058651	-77.953564	-77.935391
90/0	-78.056516	-77.955253	-77.935752
60/5	-78.105749	-77.923614	-77.878027
70/5	-78.085178	-77.939002	-77.907099
75/5	-78.074966	-77.942948	-77.919347
80/5	-78.064414	-77.942830	-77.929182
85/5	-78.058491	-77.954028	-77.934811
90/5	-78.055847	-77.955639	-77.927478
60/10	-78.104734	-77.923151	-77.877883
70/10	-78.084417	-77.940214	-77.906475
75/10	-78.074332	-77.944280	-77.918510
80/10	-78.063782	-77.950778	-77.928029
85/10	-78.057952	-77.955297	-77.933148
90/10	-78.055788	-77.956830	-77.934111
60/20	-78.099233	-77.923085	-77.875197
70/20	-78.079832	-77.941039	-77.901789
75/20	-78.070222	-77.948569	-77.912759
80/20	-78.059546	-77.952806	-77.924171
85/20	-78.054953	-77.959569	-77.923546
90/20	-78.052853	-77.964717	-77.928217
60/30	-78.087165	-77.930968	-77.868481
70/30	-78.069108	-77.949421	-77.891603
75/30	-78.057128	-77.953992	-77.899811
80/30	-78.049867	-77.963011	-77.907431
85/30	-78.044781	-77.968219	-77.912354
90/30	-78.043069	-77.97013	-77.913087

Table 2.1 CASSCF energies (a.u.) of the investigated ethylene geometries in the 60-90˚ torsion (α) and 0-30˚ pyramidalization (ϕ) range.

A number of remarkable observations can be made. First of all, for root 1 (the N state), similar behaviour can be observed at both levels of theory. Typical dipole moments along the z-axis range from 0.1 to 0.3 D at the strongly pyramidalized geometries.
These results compare qualitatively well with the results of both Brooks and Buenker et al.[10, 23]

α/ϕ	root 1	root 2	root 3
60/0	-78.321076	-78.172086	-78.118806
70/0	-78.303250	-78.174723	-78.148982
75/0	-78.295122	-78.168474	-78.163172
80/0	-78.288638	-78.172688	-78.175467
85/0	-78.285696	-78.176530	-78.183978
90/0	-78.284213	-78.178070	-78.184538
60/5	-78.320720	-78.171688	-78.118893
70/5	-78.302890	-78.159660	-78.149292
75/5	-78.294788	-78.168801	-78.163199
80/5	-78.289494	-78.166518	-78.175280
85/5	-78.285489	-78.176977	-78.183636
90/5	-78.283832	-78.178478	-78.183782
60/10	-78.319572	-78.169852	-78.118863
70/10	-78.301944	-78.161017	-78.148815
75/10	-78.293944	-78.169806	-78.162481
80/10	-78.288834	-78.174387	-78.173967
85/10	-78.284821	-78.178227	-78.180973
90/10	-78.283388	-78.179675	-78.182586
60/20	-78.314080	-78.165298	-78.116246
70/20	-78.297236	-78.168465	-78.143810
75/20	-78.289628	-78.173457	-78.155985
80/20	-78.285351	-78.178539	-78.168132
85/20	-78.280240	-78.182419	-78.161246
90/20	-78.279739	-78.184555	-78.172288
60/30	-78.302312	-78.158620	-78.106148
70/30	-78.286627	-78.169510	-78.128945
75/30	-78.280863	-78.177597	-78.138800
80/30	-78.275266	-78.183419	-78.146539
85/30	-78.271408	-78.187456	-78.146793
90/30	-78.270028	-78.188931	-78.145265

Table 2.2 CASPT2 energies (a.u.) of the investigated ethylene geometries in the 60-90˚ torsion (α) and 0-30˚ pyramidalization (ϕ) range.

For the Z and V state the behaviour is less straightforward (see also figure 2.5) As can be seen from figure 2.5, at the CASSCF level root 2 is increasingly stabilized by progressive pyramidalization after a small barrier (ϕ = 5˚) has been taken, whereas root 3 becomes increasingly destabilized, especially at larger pyramidalization angles.

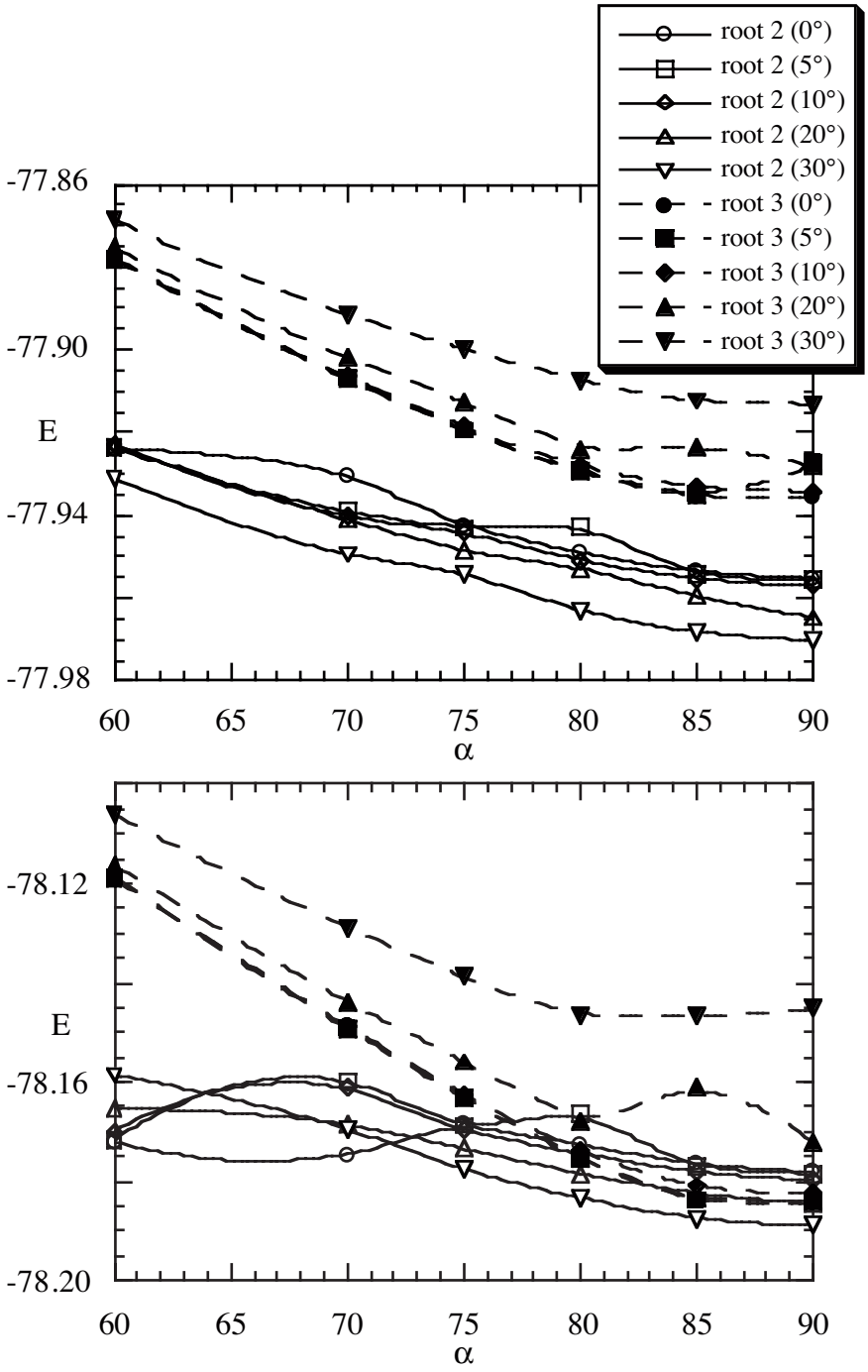

Figure 2.5 CASSCF (top plot) and CASPT2 (bottom plot) potential energy surfaces (a.u.) of root 2 (solid lines) and 3 (dashed lines) for various values of ϕ.

Although the behaviour of root 2 is in agreement with previous findings, which show that a certain amount of activation energy is required (i.e. a pyramidalization barrier has to be taken) before the pyramidalized conformations of root 2 become more stable than the planar one, the overall picture is inaccurate since a significant energy difference exists between root 2 and 3 for all conformations, even at the avoided crossing near 80˚.

This is not unexpected due to the aforementioned limitations of the CASSCF approach. In addition, truncated MCSCF wave functions tend to overcorrelate localized (polar) solutions. The occurrence of such non-degenerate polar solutions at unpyramidalized geometries not only shows that undesired, excessive mixing of the Z and V states take place, but that the expectation values of the accompanying energies are also incorrect. It will be demonstrated in the remainder of this chapter that the latter inaccuracy is largely repaired by the subsequent CASPT2 calculations.

A remarkable difference in dipole moment (μ_z) can be observed as well. Root 2 (as predicted) shows large dipole moments from 70-90˚ (around 3 Debye), whereas root 3 shows much smaller dipole moments (around 1 Debye). This is unexpected, because the antisymmetric nature of the two states involved should direct these calculations towards states having equally large dipole moments that only differ in sign. Apparently, two clearly non-orthogonal states have been obtained. An obvious solution would be to perform a so called Restricted Active Space State Interaction (RASSI) calculation[49] in which the states will be orthogonalized again. Application of this method has lead to a dramatic destabilization of the third root caused by the 'polar' nature of the orbitals. For root 2, the electron pair will effectively be localized at one of the carbons, leaving an electron hole at the other. In the RASSI, root 3 will have both electrons projected in the orbitals of the electron hole which are likely to be very contracted. This will lead to a large electron-electron repulsion term in the energy expression for this state.

In addition, it is questionable whether such a procedure is really necessary in this case. Consider the following hypothetical situation. On assuming a small transition probability between the two PES of interest, an excited state population can pass the crossing area several times without actually crossing to the lower surface. In this situation, the population will remain at the higher of the two potential energy surfaces on progressive twisting. As demonstrated, this surface becomes destabilized by pyramidalization. This is reflected by the lower expectation value of the dipole moments for this state. In fact, if state averaging (i.e. the moderate mixing of root 2 into the CASSCF optimization of root 3) is applied, the magnitude of these dipole moments as well as the difference between the dipole moments of root 2 and 3 is significantly reduced. Therefore, this non-orthogonality can be interpreted as a reflection of the aforementioned difference in PES behaviour. A more elaborate discussion on this difference in behaviour can be found in chapter 5.

At the CASPT2 level the picture is more in accordance with previous work. The overcorrelation of root 2 with respect to root 3 gets repaired and their near-degeneracy at planar or moderately pyramidalized near-perpendicular geometries is restored again, even though the expectation values of the dipole moments do not change significantly from the CASSCF ones. However, some suspicious looking energy barriers can be observed in the various potential energy surfaces in figure 2.5. Especially the PES of root 3 at $\phi = 20^\circ$ appears to be erratic in the vicinity of the perpendicular geometry. This is probably caused by the fact that severe state averaging (ratio 1:4 for root 2 : root 3) was required to reach convergence for the CASSCF calculation. The large amount of root 2 behaviour may have caused the overstabilization of this strongly pyramidalized geometry.

Focussing on the larger picture at the perpendicular geometry, the observation can be made that only at large pyramidalization angles ($\phi = 30^\circ$) root 2 becomes more

α/ϕ	root 1	root 2	root 3
CASSCF			
90/0	-234.2236870	-234.1229404	-234.0995915
90/10	-234.2264883	-234.1230315	-234.0954081
90/20	-234.2124947	-234.117909	-234.0796808
90/30	-234.1655431	-234.0862198	-234.022427
CASPT2			
90/0	-234.9978758	-234.8962502	-234.9065978
90/10	-234.9946143	-234.8964841	-234.9007436
90/20	-234.9818408	-234.8924526	-234.8763497
90/30	-234.9392147	-234.8650318	-234.8126322

Table 2.3 CASSCF and CASPT2 energies (a.u.) of various pyramidalization angles ϕ of perpendicular TME

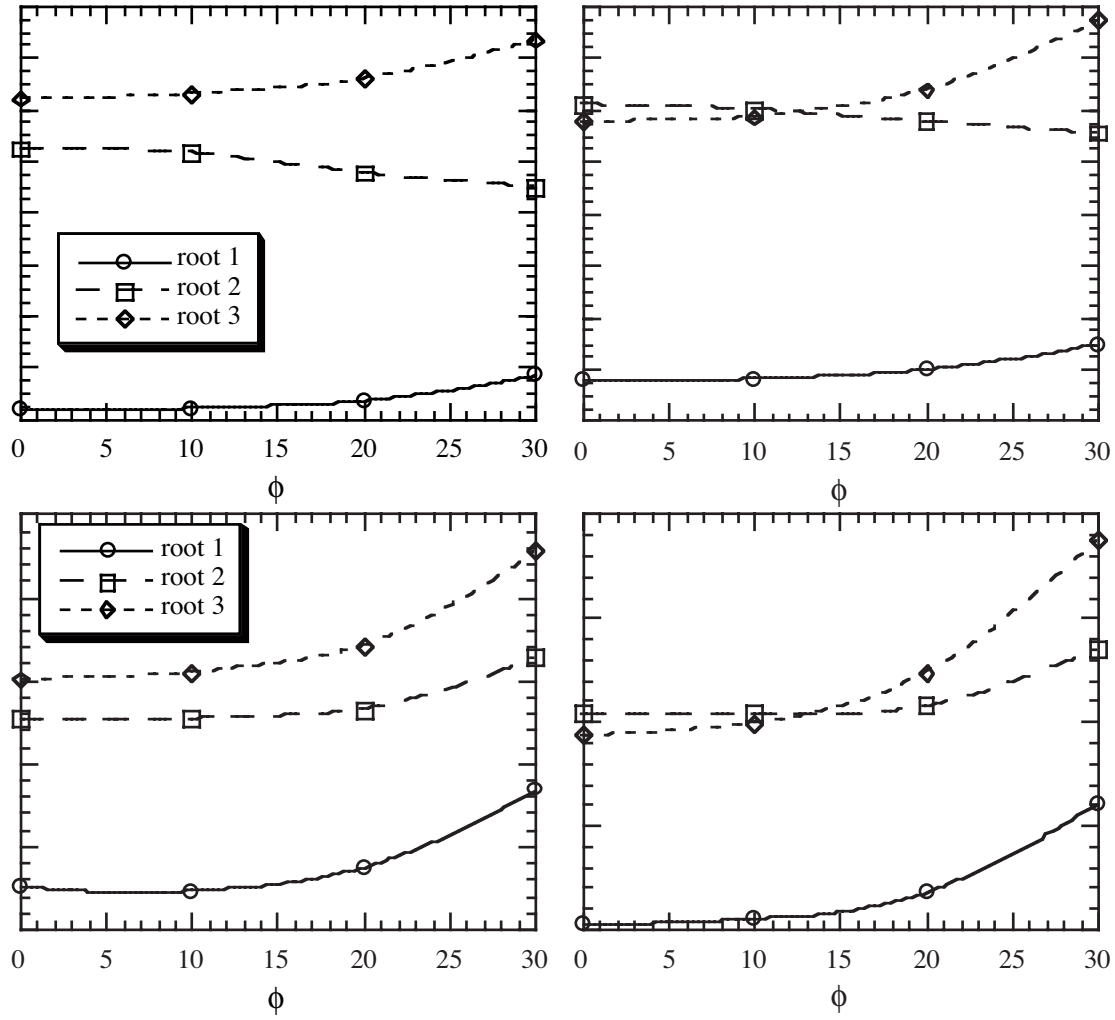

Figure 2.6 CASSCF (left plot) and CASPT2 (right plot) energies (a.u.) of perpendicular ethylene (top plots) and TME (bottom plots) at the investigated values of ϕ.

stabilized than the planar root 3, which is in good agreement with the findings of Brooks et al. at the CISD level of theory[10].

In general, the CASPT2 wave functions appear to reproduce the expectation values of the energies of the excited states of such systems reasonably well even though the expectation values of the dipole moments are still unrealistic. This is not surprising, since it cannot be expected that second-order perturbation theory can repair the strongly polarized input wave functions based on an extensive CAS. However, the fact that potential energy surfaces similar to previous work are reproduced justifies an attempt to investigate the pyramidalization behaviour of TME at the perpendicular geometry. These results are presented in table 2.3 and visualized in figure 2.6.

When comparing the TME and ethylene results, it becomes apparent that the qualitative behaviour of the CASSCF and CASPT2 wave functions is quite similar. For both ethylene and TME the near-degeneracy of root 2 and 3 (the Z and V state) is best reproduced at the CASPT2 level of theory. In fact, for both systems a crossing of the Z and V surface is predicted near $\phi = 13^{\circ}$. This is a clear indication of the generic nature of the sudden polarization effect in D_2-symmetrical alkenes.

However, there is a striking difference in the PES behaviour of the two systems. Where root 2 gets stabilized on progressive pyramidalization in the ethylene case, the corresponding root in the TME case lacks this stabilization. Even though both the CASSCF and CASPT2 PES of root 2 of TME are rather flat for the more moderate values of ϕ, at which in fact a shallow minimum can be observed (see table 2.3), at progressive pyramidalization all three roots become significantly destabilized. This can be explained by the nature of the substituents on the carbon double bond; the small hydrogens can be pushed towards each other without significantly increasing repulsion between them. The more bulky methyl groups are much more prone to 'feeling' the repulsion, as schematically depicted in figure 2.2. Therefore, this contribution to the state energy will dominate the PES behaviour when ϕ becomes large enough. This effect is even more dramatic for root 3, since both pyramidalization as well as repulsion destabilize the state, leading to a steep PES for this state in the TME case.

These observations raise the suspicion that internal symmetry breaking may not be the main driving force in the occurrence of polarized, zwitterionic excited states of D_2-symmetrical alkenes, since for large substituents (like for instance the phenyl groups at TPE) the steric hindrance is likely to prevent significant stabilization by pyramidalization due to the expected large amount of introduced steric hindrance.

Nevertheless, large excited state dipole moments have been reported for systems like TPE[31, 50]. Interestingly, these experimentally observed polar states have always been reported for alkenes in the condensed phase. In addition, solvent dependent behaviour has been observed in many cases[31, 40, 42, 43]. This justifies the question whether external symmetry breaking, like an intrisically low-symmetry solvent shell, is capable of providing a large enough perturbation of the ethylenic wave function in order to produce effective symmetry breaking. In other words, is a solvent solely capable of polarizing ethylenic excited states at near-perpendicular geometries ?

The answer to this question will be given in the remainder of this thesis.

2.5 Conclusion

In this chapter, the simultaneous torsion and pyramidalization of ethylene at in the vicinity of the perpendicular geometry as well as the pyramidalization of TME at the perpendicular geometry has been investigated at the CASPT2 level of theory in an attempt to study the sudden polarization effect. It has been explained that the description of this phenomenon by these types of wave functions is not necessarely the best choice, since truncated MCSCF expansions lead to (over)polarized solutions of the excited states of interest in the vicinity of the avoided crossing between the $a^2 + b^2$ (Z) and $a^2 - b^2$ (V) state.

It has been shown by comparing the ethylene results with earlier reported work that the relative CASSCF energy differences between the excited states of interest were inaccurate. This has been attributed to the fact that the polarized first excited state benefits more from the (unwanted) wave function polarization than its antisymmetric counterpart. The correct behaviour was reproduced at the CASPT2 level of theory, however. At this level of theory, the near degeneracy of the two states was reproduced, indicating that as far as relative energies are concerned, the CASPT2 method provided results bearing some physical significance. Furthermore, the stabilization by selective pyramidalization of the lowest of the two surfaces involved in the avoided crossing was established as well, also in good agreement with previously reportes studies.Therefore, it was concluded that as far as the shape of the ethylenic potential energy surfaces of interest is concerned, the CASPT2 level of theory is capable of reproducing them with acceptable accuracy.

On the basis of this positive conclusion, the selective pyramidalization of TME at the perpendicular geometry has also been investigated at the CASPT2 level of theory. The aforementioned differences in the CASSCF and CASPT2 energies of the ethylene PES were also observed in the TME case, as can be seen in figure 2.6. This indicates the similar excited state behaviour of the two alkenes at the perpendicular geometry. However, a significant difference in the PES shape of the lowest of the two surfaces involved in the avoided crossing (i.e. root 2) has been observed. In contrast with the ethylene case, where this PES became stabilized as a result of this symmetry lowering perturbation, the TME PES of root 2 was significantly destabilized at larger pyramidalization angles. This has been explained by the much larger increase in steric hindrance between the two methyl groups with respect to the hydrogens when these groups are forced together by the pyramidalization as schematically depicted in figure 2.2. This remarkable observation has led to the conclusion that the widely accepted theory, in which the intramolecular lowering of the molecular symmetry (i.e selective pyramidalization) is held mainly responsible for the formation of ethylenic excited states with large dipole moments, might not hold for larger D_2-symmetrical alkenes.

2.6 References

1. R.S. Mulliken, Phys. Rev., **41**, 751-758 (1932).
2. L. Salem and C. Rowland, Angew. Chem., Int. Ed. Engl., **11**, 92-111 (1972).
3. J.A. Marshall, Science, **170**, 137-141 (1970).
4. C.E. Wulfman and S. Kumei, Science, **172**, 1061 (1971).
5. C.E. Wulfman and G.C. Hyatt, Proc. Indian Acad. Sci. (Chem. Sci.), **107**, 813-823 (1985).
6. V. Bonacic-Koutecky, P. Bruckmann, P. Hiberty, J. Koutecky, C. Leforestier and L. Salem, Angew. Chem., Int. Ed. Engl., **14**, 575-576 (1975).
7. V. Bonacic-Koutecky, J. Cizek, D. Döhnert and J. Koutecky, J. Chem. Phys., **69**, 1169-1176 (1978).
8. V. Bonacic-Koutecky, J. Am. Chem. Soc., **100**, 396-404 (1978).
9. V. Bonacic-Koutecky, R.J. Buenker and S.D. Peyerimhoff, J. Am. Chem. Soc., **101**, 5917-5922 (1979).
10. B.R. Brooks and H.F Schaefer III, J. Am. Chem. Soc., **101**, 307-311 (1979).
11. S. Ramasesha and I.D.L. Albert, Chem. Phys., **142**, 395-402 (1990).
12. R.W.J. Zijlstra, A.H. de Vries and P.Th. van Duijnen, Chem. Phys., **204**, 439-446 (1996).
13. A. Szabo and N.S. Ostlund, *Modern Quantum Chemistry*, Macmillan Publishing Co. Inc., New York, 1982.
14. B.O. Roos Ed., *Lecture Notes in Quantum Chemistry*, Springer-Verlag, Heidelberg, 1992.
15. B.O. Roos, P.R. Taylor and P.E.M. Siegbahn, Chem. Phys., **48**, 157-173 (1980).
16. B.O. Roos, in: Ab Initio Methods in Quantum Chemistry II, Ed: K. P. Lawley, John Wiley & Sons Ltd., New York, 1987.
17. P-Å Malmqvist, A. Rendell and B.O. Roos, J. Phys. Chem., **94**, 5477-5482 (1990).
18. C. Möller and M.S. Plessett, Phys. Rev., **34**, 618 (1934).
19. K. Andersson, P-Å Malmqvist, B.O. Roos, A.J. Sadlej and K. Wolinski, J. Phys. Chem., **94**, 5483-5488 (1990).
20. K. Andersson, P-Å. Malmqvist and B.O. Roos, J. Chem. Phys., **96**, 1218-1226 (1992).
21. H.-J. Werner and P.J. Knowles, J. Chem. Phys., **89**, 5803-5814 (1988).
22. B.O. Roos and K. Andersson, Chem. Phys. Lett., **245**, 215-223 (1995).
23. R.J. Buenker, V. Bonacic-Koutecky and L. Pogliani, J. Chem. Phys., **73**, 1836-1849 (1980).
24. V. Bonacic-Koutecky, L. Pogliani, M. Persico and J. Koutecky, Tetrahedron, **38**, 741-751 (1982).
25. P. Bruckmann and L. Salem, J. Am. Chem. Soc., **98**, 5037-5038 (1976).
26. C.M. Meerman-van Benthem, H.J.C. Jacobs and J.J.C. Mulder, Nouv. J. Chim., **2**, 123-127 (1977).
27. G. Orlandi, P. Palmieri and G. Poggi, J. Am. Chem. Soc., **101**, 3492-3497 (1979).
28. I.D.L. Albert and S. Ramasesha, J. Phys. Chem., **94**, 6540-6543 (1990).

29. M. Merchán and R. González-Luque, J. Chem. Phys., **106**, 1112-1122 (1997).
30. L. Salem, Acc. of Chem. Res., **12**, 87-92 (1979).
31. W. Schuddeboom, S.A. Jonker, J.M. Warman, M.P. de Haas, M.J.W. Vermeulen, W.F. Jager, B. de Lange, B.L. Feringa and R.W. Fessenden, J. Am. Chem. Soc., **115**, 3286-3290 (1993).
32. G. Orlandi and W. Siebrand, Chem. Phys. Lett., **14**, 19-22 (1972).
33. G. Orlandi and W. Siebrand, Chem. Phys. Lett., **80**, 399-403 (1981).
34. A. Farazdel, M. Dupuis, E. Clementi and A. Aviram, J. Am. Chem. Soc., **112**, 4206-4214 (1990).
35. C. Zener, Proc. Roy. Soc. London, A, **137**, 696-702 (1932).
36. M. Persico, J. Am. Chem. Soc., **102**, 7839-7845 (1980).
37. I.D. Petsalakis, G. Theodorakopoulos, C.A. Nicolaidis, R.J. Buenker and S.D. Peyerimhoff, J. Chem. Phys., **81**, 3161-3167 (1984).
38. I.D. Petsalakis, G. Theodorakopoulos and C.A. Nicolaidis, J. Chem. Phys., **81**, 5952-5956 (1984).
39. R. Broer-Braam, *Localized orbitals and broken symmetry in molecules*, Ph.D. thesis, University of Groningen, 1981.
40. P.F. Barbara, S.D. Rand and P.M. Rentzepis, J. Am. Chem. Soc., **103**, 2156-2162 (1981).
41. C.L. Schilling and E.F. Hilinski, J. Am. Chem. Soc., **110**, 2296-2298 (1988).
42. Y-P. Sun and C.E. Bunker, J. Am. Chem. Soc., **116**, 2430-2433 (1994).
43. R.W.J. Zijlstra, P. Th. van Duijnen, B.L. Feringa, T. Steffen, K. Duppen and D.A. Wiersma, J. Phys. Chem. A, **101**, 9828-9836 (1997).
44. K. Andersson, M.R.A. Blomberg, M.P. Fülscher, V. Kellö, R. Lindh, P.-Å. Malmqvist, J. Noga, J. Olsen, B.O. Roos, A.J. Sadlej, P.E.M. Siegbahn, M. Urban and P.-O. Widmark, *Molcas version 3*, University of Lund, Sweden, 1994.
45. K. Pierloot, B. Dumez, P-O. Widmark and B.O. Roos, Theor. Chim. Acta, **90**, 87-114 (1995).
46. R.J. Buenker and S.D. Peyerimhoff, Chem. Phys., **9**, 75-89 (1976).
47. C.C. Ballard, M. Hada and H. Nakatsuji, Bull. Chem. Soc. Japan, **69**, 1901-1906 (1996).
48. J.D. Watts, S.R. Gwaltney and R.J. Barrett, J. Chem. Phys., **105**, 6979-6988 (1996).
49. P.-Å. Malmqvist and B.O. Roos, Chem. Phys. Lett., **155**, 189-194 (1989).
50. J. Morais, J. Ma and M.B. Zimmt, J. Phys. Chem., **95**, 3885-3889 (1991).